

clouds originate at the focus and expand to a diameter of about 2 in. in a few seconds, providing a simple method for distinguishing between breakdown and prebreakdown ionization. Sequential photographs were taken of these clouds within a few minutes after breakdown occurred, and they are shown in Fig. 1. This breakdown followed by cloud effects was observed throughout the cloud chamber independent of the ion-sensitive region. The clouds also completely overshadowed any condensation due to ionization.

Photographs of breakdown illuminated by the plasma radiation were obtained as shown in Fig. 2. In this figure several plasma spots appear to be produced near the focus of the lens. The number of spots varied from one to three on successive laser shots. This can be ascribed to multimode oscillation of the ruby rod, a subject of current controversy.²³ The spectrum of these plasmas included a continuum with peak optical intensity in the blue region, as observed through a diffraction grating.

Our interpretation of the breakdown phenomena observed in the cloud chamber agrees with that of Haught.⁸ Following laser breakdown, about half of the laser energy is absorbed into a focal volume of about one cubic millimeter. Heat diffuses outward from the focus and upsets the normal equilibrium conditions in the chamber. Condensation is produced in the form of visible clouds which do not resemble droplets nucleated by charged particles. The clouds were, therefore, interpreted as precipitation of supersaturated vapors due to high local-temperature gradients produced by the breakdown phenomena.

Experiments are in progress to measure the prebreakdown ionization quantitatively as a function of laser power and time to determine if the electron density increases exponentially in this region as Phelps predicts.

The authors wish to acknowledge the benefit of discussions with Professor Jacques Ducuing of Massachusetts Institute of Technology and with A. V. Phelps of Westinghouse Research Laboratories.

Stark Broadening of an Ionized-Mercury Line

KIYOSHI MURAKAWA

*Institute of Space and Aeronautical Science, University of Tokyo,
Komaba-machi, Meguro-ku, Tokyo, Japan*

(Received 23 July 1965; revised manuscript received 17 December 1965)

The profile of the line Hg II $\lambda 3984$ emitted from a high-current mercury arc of mean temperature 6500 ± 800 °K and with electron density $(2.6 \pm 0.7) \times 10^{16}$ /cc was studied with a Fabry-Perot etalon. The full half-width of a single even-isotope component due to Stark broadening was found to be 0.39 ± 0.08 cm⁻¹, in which the broadening due to the Doppler effect is subtracted, and the shift relative to an unperturbed line was found to be -0.013 ± 0.010 cm⁻¹. The shift can be interpreted to be due to distant collisions of the perturbing electrons; approximately 90% of the width was found to be due to close collisions.

A HIGH-current mercury arc within a quartz tube of vertical type fed by 200 V ac was viewed in the horizontal direction and was studied spectroscopically. The temperature was determined by the method described by Göing,¹ and the mean temperature of the luminous part was found to be 6500 ± 800 °K, from which the mean velocity of the plasma electrons is calculated to be $\langle v \rangle = 4.4 \times 10^7$ cm/sec. The mean electron density was obtained by observing the series $6^3P_1 - n^3D$; the line $\lambda 2352$ ($n=10$, $n^*=6.95$) was still recognized as a line, but the next member ($n=11$, $n^*=7.95$) was found to form a continuous band with higher members. Since Inglis-Teller's formula

$$\log_{10} N = 23.26 - 7.5 \log_{10} n_m$$

is based on hydrogen wave functions, one puts n_m^*

(instead of n_m)² in this formula, namely

$$n_m^* = (6.95 + 7.95)/2 = 7.45.$$

In this way one gets $N = 5.2 \times 10^{16}$, and assuming that $N_e = N$, one obtains $N_e = 2.6 \times 10^{16}$. This is probably accurate to $\pm 30\%$.

The profile of the ion line Hg II $\lambda 3984$ (classified by Paschen³ as $5d^96s^2 \ ^2D_{5/2} - 5d^{10}6p^2 \ ^2P_{3/2}$) was studied with a Fabry-Perot etalon with a spacer in the range 1.0–2.0 mm. The same line emitted from a liquid-air-cooled hollow-cathode discharge tube was chosen as an unperturbed standard.⁴ The line $\lambda 3984$ has a hyperfine

² D. R. Hartree, Proc. Cambridge Phil. Soc. **24**, 89 (1928), especially Sec. 5.

³ F. Paschen, Sitzber. Preuss. Akad. Wiss. Physik. Math. Kl. **32**, 3 (1928).

⁴ K. Murakawa, Sci. Papers Inst. Phys. Chem. Research (Tokyo) **18**, 299 (1932); S. Mrozowski, Phys. Rev. **57**, 207 (1940).

¹ W. Göing, Z. Physik **131**, 603 (1952).

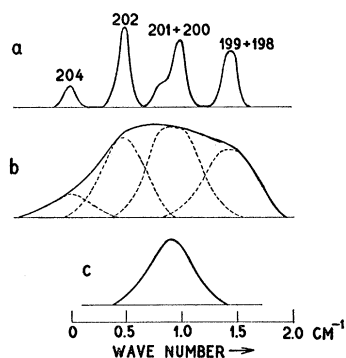


FIG. 1. Profile of Hg II $\lambda 3984$ observed with a 2-mm etalon. (a) Liquid-air-cooled hollow cathode discharge. 199+198 appears as a single component with a full half-width which is larger by 0.04 cm^{-1} than that of 204 or 202. 201+200 can be resolved by a graphical method; 201 has a full half-width which is larger by 0.03 cm^{-1} than that of 204 or 202. (b) High-current mercury arc lamp. The profile from which the continuous background intensity is subtracted is given. Decomposition of the observed profile was done in such a way that the areas under 204, 202, 201, 200, and 199+198 are proportional to the respective natural abundances and the half-widths of 204, 202, 200, 201— 0.03 cm^{-1} , and 199+198— 0.04 cm^{-1} are equal, and that their shapes are similar. In this figure the superposed 201+200 is drawn for brevity. (c) Profile of a single even-isotope component deduced from (b).

structure due to isotope shift and splittings of the odd-isotope components; the components 204 and 202 are fairly well isolated and are suited for profile measurements [Fig. 1(a)]. Figure 1(b) shows the profile of $\lambda 3984$ emitted from the high-current arc, the dotted curve representing the decomposed profile of each isotope component, and the profile of the components 204 or 202 can be well represented by Fig. 1(c). This has the (full) half-width $0.46 \pm 0.04 \text{ cm}^{-1}$. On the other hand the instrumental width (2-mm etalon) was found to be 0.08 cm^{-1} , so the true width of the profile is $0.42 \pm 0.05 \text{ cm}^{-1}$. The thermal Doppler width was calculated to be $0.10 \pm 0.02 \text{ cm}^{-1}$, leaving a true Stark width of $0.39 \pm 0.08 \text{ cm}^{-1}$. The shift of each component relative to an unperturbed component was observed to be $-0.013 \pm 0.010 \text{ cm}^{-1}$ (red shift).

When the mercury ion is placed in a uniform electric field of intensity F , the line $\lambda 3984$ suffers a shift $\Delta\nu$. The constant γ defined by

$$\Delta\nu = \gamma F^2$$

was calculated by means of formulas that were deduced for the case of alkali atoms.⁵ The radial integrals were calculated by the Coulomb approximation method due to Bates and Damgaard.⁶ Five components were obtained, but if one assumes that they are not resolved, then one gets an effective constant $\gamma = -7.8 \times 10^{-8}$

⁵ K. Murakawa and M. Yamamoto, J. Phys. Soc. Japan **20**, 1057 (1965).

⁶ D. R. Bates and A. Damgaard, Phil. Trans. Roy. Soc. (London) **242**, 101 (1949).

$\text{cm}^{-1}/(\text{kV}/\text{cm})^2$, whose sign is in agreement with the above-mentioned observation.

The recently refined theory^{7,8} predicts, in our case, a shift of the order of -10^{-2} cm^{-1} contributed by distant collisions. The observed shift $-0.013 \pm 0.010 \text{ cm}^{-1}$ is at least in qualitative agreement with the theory. However, the plasma polarization shift suggested by Berg *et al.*⁹ seems to play an unimportant role in the case of Hg II $\lambda 3984$, because it predicts a large blue shift. Close collisions disturb completely the phase of the emitted electromagnetic wave and therefore contribute nothing to the shift.

The theory^{7,8} predicts that the distant collisions contribute a width of the order of $2 \times 10^{-2} \text{ cm}^{-1}$. If one subtracts this amount from the observed Stark width, one gets $0.36 \pm 0.10 \text{ cm}^{-1}$, which must be ascribed to close collisions. If this is interpreted by the Lorentz-Weisskopf formula

$$w = \rho_{\min}^2 N_e \langle v \rangle / c \text{ cm}^{-1},$$

the cutoff impact parameter ρ_{\min} plays the most important part, together with the electron density N_e and the average velocity $\langle v \rangle$. At present there is no adequate theory that predicts ρ_{\min} which is in agreement with the observation, but if one determines ρ_{\min} by the formula deduced by an elementary consideration [see Eq. (3) of Ref. 10]¹¹

$$\rho_{\min} = e^2 a_0 n^{*2} / (Z \langle v \rangle \hbar)$$

(the notations have their usual meanings; Z is 1, 2, 3, ... for neutral, singly ionized, doubly ionized, ... atom, respectively), one obtains $\rho_{\min} = 6.3 \times 10^{-8} \text{ cm}$, and the predicted full half-width (due to close collisions) becomes 0.31 cm^{-1} , which is in agreement with the observation ($0.36 \pm 0.10 \text{ cm}^{-1}$), although it is at present not so clear why such a determination of ρ_{\min} is better than others.

We may conclude that as a practice (experimental method), investigation of the Stark broadening of the lines of ionized atoms is the most suited for clarifying the mechanism of close collisions, owing to the strong Coulomb attraction between ionized atoms and electrons which is not the case for neutral atoms.

⁷ H. Margenau and M. Lewis, Rev. Mod. Phys. **31**, 569 (1959).

⁸ H. R. Griem, M. Baranger, A. C. Kolb, and G. Oertel, Phys. Rev. **125**, 177 (1962). According to these authors the cutoff impact parameter ρ_{\min} is to be determined by their Eq. (3.16). But Yamamoto (Ref. 9) has shown that, at least in the case of Ca II, the value of ρ_{\min} determined in this way is too small to account for the observed Stark width.

⁹ H. F. Berg, A. W. Ali, R. Lincke, and H. R. Griem, Phys. Rev. **125**, 199 (1962).

¹⁰ M. Yamamoto, following paper, Phys. Rev. **146**, 137 (1966).

¹¹ This equation is approximately the same as Eq. (3.13) of Ref. 8, but they obtained this equation as the high-temperature limit of their Eq. (3.16), namely, in the case in which strong collisions are negligible.